

Article

Formation and Intramolecular Capture of α -Imino Gold Carbenoids in the Au(I)-Catalyzed [3 + 2] Reaction of Anthranils, 1,2,4-Oxadiazoles, and 4,5-Dihydro-1,2,4-Oxadiazoles with Ynamides

Ioannis Stylianakis ¹, Iraklis Litinas ¹, Antonios Kolocouris ^{1,*}  and Carlos Silva López ^{2,*} 

¹ Laboratory of Medicinal Chemistry, Section of Pharmaceutical Chemistry, Faculty of Pharmacy, National and Kapodistrian University of Athens Panepistimiopolis Zografou, 15771 Athens, Greece

² Departamento de Química Orgánica, Facultad de Química, Universidad de Vigo, Campus Lagoas-Marcosende, 36310 Vigo, Spain

* Correspondence: author: ankol@pharm.uoa.gr (A.K.); carlos.silva@uvigo.es (C.S.L.)

Abstract: α -Imino gold carbenoid species have been recognized as key intermediates in a plethora of processes involving gold-activated alkynes. Here, we explored the pathways of the Au(I)-catalyzed [3 + 2] reaction between the mild nucleophiles: anthranil, 1,2,4-oxadiazole, or 4,5-dihydro-1,2,4-oxadiazole, and an ynamide, PhC \equiv C-N(Ts)Me, proceeding via the formation of the aforementioned α -imino gold carbene intermediate which, after intramolecular capture, regioselectively produces 2-amino-3-phenyl-7-acyl indoles, *N*-acyl-5-aminoimidazoles, or *N*-alkyl-4-aminoimidazoles, respectively. In all cases, the regioselectivity of the substituents at 2, 3 in the 7-acyl-indole ring and 4, 5 in the substituted imidazole ring is decided at the first transition state, involving the attack of nitrogen on the C1 or C2 carbon of the activated ynamide. A subsequent and steep energy drop furnishes the key α -imino gold carbene. These features are more pronounced for anthranil and 4,5-dihydro-1,2,4-oxadiazole reactions. Strikingly, in the 4,5-dihydro-1,2,4-oxadiazole reaction the significant drop of energy is due to the formation of an unstable α -imino gold carbene, which after a spontaneous benzaldehyde elimination is converted to a stabilized one. Compared to anthranil, the reaction pathways for 1,2,4-oxadiazoles or 4,5-dihydro-1,2,4-oxadiazoles are found to be significantly more complex than anticipated in the original research. For instance, compared to the formation of a five-member ring from the α -imino gold carbene, one competitive route involves the formation of intermediates consisting of a four-member ring condensed with a three-member ring, which after a metathesis and ring expansion led to the imidazole ring.

Keywords: Au(I) catalysis; [3 + 2] addition; α -imino gold carbene; N-heterocycles; alkyne activation



Citation: Stylianakis, I.; Litinas, I.; Kolocouris, A.; Silva López, C. Formation and Intramolecular Capture of α -Imino Gold Carbenoids in the Au(I)-Catalyzed [3 + 2] Reaction of Anthranils, 1,2,4-Oxadiazoles, and 4,5-Dihydro-1,2,4-Oxadiazoles with Ynamides. *Catalysts* **2022**, *12*, 915. <https://doi.org/10.3390/catal12080915>

Academic Editor: C. Heath Turner

Received: 1 August 2022

Accepted: 11 August 2022

Published: 19 August 2022

Publisher's Note: MDPI stays neutral with regard to jurisdictional claims in published maps and institutional affiliations.



Copyright: © 2022 by the authors. Licensee MDPI, Basel, Switzerland. This article is an open access article distributed under the terms and conditions of the Creative Commons Attribution (CC BY) license (<https://creativecommons.org/licenses/by/4.0/>).

1. Introduction

The first reported example of a gold-catalyzed heterocyclic synthesis invoking the participation of α -imino gold carbene complexes can be attributed to Toste in the Au(I)-catalyzed acetylene Schmidt reaction of homopropargyl azides acting as nitrene transfer reagents to furnish substituted pyrroles in 2005 [1]. For this intermediate, Goddard and Toste [2] suggested a three-center, four-electron σ -bond due to donation to the empty 6s orbital of gold from the occupied orbitals at the ligand and the carbene carbon atom, as well as two orthogonal π -electron density back-donations from filled gold 5d orbitals to π -acceptor orbitals in the carbene carbon atom and on the ligand. As a result, they suggested that “the reactivity in gold(I)-coordinated carbenes is best accounted for by a continuum ranging from a metal-stabilized singlet carbene to a metal-coordinated carbocation”. Additionally, the bond order in gold(I) carbene complexes is typically close to one (or even less), and therefore, the Au=C representation is not accurate, although it may be convenient mainly for mechanistic purposes [3–7]. Ynamides, which are strongly polarized alkynes, [8]

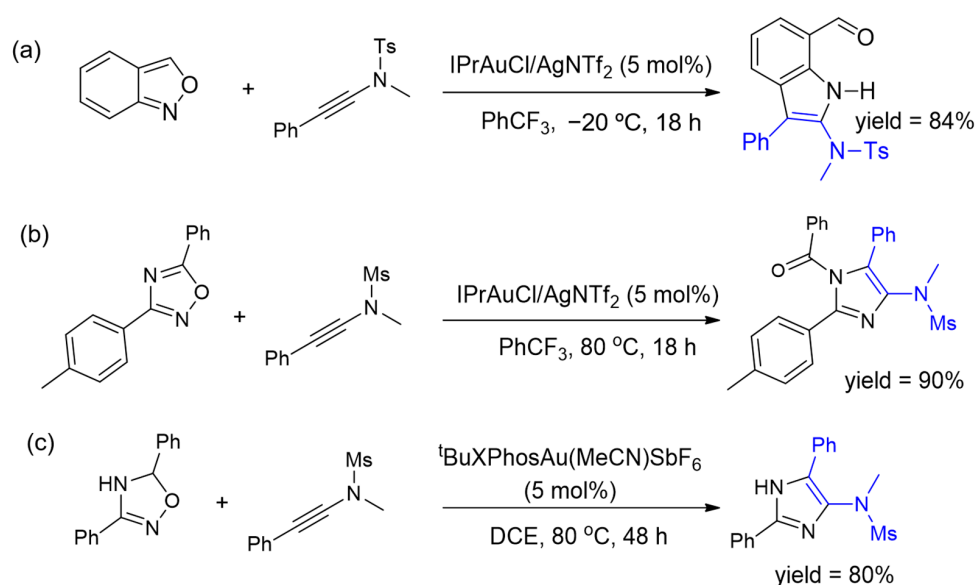
have been established as an extremely powerful tool for the rapid and versatile assembly of structurally complex *N*-containing molecules [9–12] with gold-catalyzed reactions [13]. In such a reaction, the participation of α -imino gold carbene intermediates is carried out through their capture by diverse types of nucleophiles.

In parallel, transition metal-catalyzed annulation reactions of anthranils or, generally, isoxazoles after ring opening have contributed greatly to producing functionalized heterocyclic derivatives and complex molecules [14]. The anthranils and isoxazoles operate as electrophilic aminating reagents in these reactions through a selective N–O bond cleavage and provide a powerful platform for C–N bond formation and *N*-heterocycle synthesis [15]. In the presence of gold catalysts, these species could serve as mild nucleophiles to attack the activated alkynes and to form α -imino gold carbene species. Indeed, various novel annulation reactions by Liu and Hashmi have recently been developed, leading to pharmaceutically relevant heterocycles [16,17]. Ye et al. reported a cationic gold-catalyzed synthesis of 2-aminopyrroles through a [3 + 2] annulation between ynamides and 3,5-disubstituted isoxazoles, which was postulated to proceed via an α -imino gold carbene intermediate. Interestingly, in the case of trisubstituted isoxazoles, fully substituted 2-aminopyrroles are obtained upon deacylation under the same conditions. When starting isoxazoles are fully substituted, 2-aminopyrroles non-acylated at position 4 are formed as unique reaction products in moderate to excellent yields. Overall, this is an atom-economic formal [3 + 2] cycloaddition process for the preparation of a wide scope of synthetically useful tetrasubstituted pyrroles. A plausible mechanism was proposed based on experimental observations and DFT calculations. After triple bond activation, N–O bond cleavage of isoxazole leads to the key α -imino gold carbenoid intermediate, followed by intramolecular 1,5-cyclization to produce Au(I)-ligated 3H-pyrrole. Subsequent ligand exchange with another ynamide yields 3H-pyrrole followed by an isomerization by a sigmatropic H-migration to afford the desired 2-amino pyrrole.

In 2016, Hashmi published on the remarkable reactivity of the weak nucleophile anthranil with activated terminal alkynes (including ynamides) in the presence of a Au(I) catalyst (Scheme 1a) [16]. The scope of this chemistry was extended in 2018 to non-polarized terminal alkynes and internal alkynes [18]. In these reactions, an α -imino gold carbene intermediate is formed which furnishes, after a C–H insertion step, the 7-acylindoles and the *N*-doped polycyclic aromatic hydrocarbons (PAHs), respectively, in an expedient and atom-economical process. Hashmi also showed that this chemistry can provide quinoline-embedded polyazaheterocycles and 2-aminopyrroles when Au(III) is used as catalyst [19]. In 2016 Ballesteros added a three-component synthesis to this family, with the preparation of 2-imidazolyl-1-pyrazolylbenzenes from 1-propargyl-1*H*-benzo-triazoles, non-polarized terminal alkynes, and nitriles through α -imino gold carbenoids [20].

This chemistry was recently extended to oxadiazoles, which allowed the synthesis of *N*-acylimidazoles through the formation of an α -imino gold carbene in the Au(I) catalyzed [3 + 2] reaction of 1,2,4-oxadiazoles (Scheme 1b) [21]. This reaction also occurs with total atom economy as the acyl group remains a part of oxadiazoles.

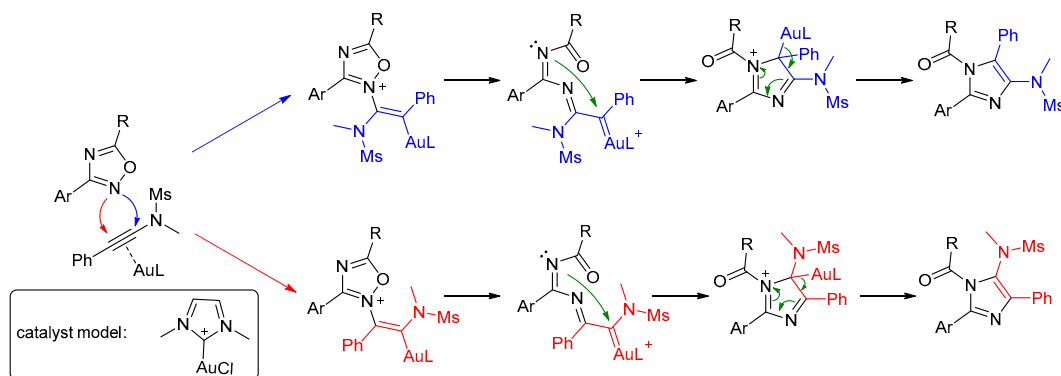
The same type of reactivity took place in the Au(I) catalyzed [3 + 2] reaction of dihydrooxadiazoles as nitrene transfer reagents reported by Liu in 2017 (Scheme 1c), which used 4,5-dihydro-1,2,4-oxadiazoles and ynamides providing *N*-R-5-4-aminoimidazoles (R=H, alkyl, aryl) [22]. It is noteworthy that several synthetic methods are available for *N*- or *C*-substituted imidazoles, [23] but only a few methods have been reported for the preparation of aminoimidazoles and derivatives [24–27]. Moreover, although 4-aminoimidazole derivatives present an interesting biological activity profile [28–31], existing synthetic methods for their preparation are limited [21,22,32].



Scheme 1. Au(I)-catalyzed reaction of anthranil (a), 1,2,4-oxadiazoles (b), or 4,5-dihydro-1,2,4-oxadiazoles (c) with ynamides forming 2-amino-3-phenyl-7-acyl indoles, *N*-acyl-4-aminoimidazoles, or *N*-*H*-4-aminoimidazoles, respectively.

As a continuation of our efforts to gain a deeper insight into the intricacies of gold-mediated transformations [3,33–45] and particularly reaction mechanisms including gold carbenes [13,16–22,46], here we carried out a thorough investigation of the reaction mechanism of the Au(I)-catalyzed [3 + 2] reaction of the mild nitrogen nucleophiles anthranil, 1,2,4-oxadiazole, and 4,5-dihydro-1,2,4-oxadiazole with ynamides. We paid particular attention to the formation of the α -imino gold carbene intermediate, the regioselectivity of these reactions which can afford 7-acyl-2-amino-indoles substituted at 2-, or/and 3-position, and 4-aminoimidazoles, respectively, as well as to the difference in reactivity between aromatic and non-aromatic substrates (oxadiazole vs. dihydrooxadiazole).

We assumed that the general mechanism for the three protocols could be analogous, according to the similarities in the structures of the three nucleophiles, and that the key feature in this reactivity is the oxime fragment embedded in the heterocyclic moiety [47–49]. With that assumption in mind, and driven by our recent exploration of anthranil chemistry [50], we anticipated a reaction pathway for the oxadiazoles involving (Scheme 2): (1) Au(I) activation of the alkyne, (2) nucleophilic attack by the oxime nitrogen onto the activated alkyne, (3) N-O cleavage and formation of the key α -imino gold carbene intermediate, (4) cyclization of the α -imino gold carbene intermediate via an intramolecular nucleophilic attack, and (5) deauration leading to the final heterocycle.



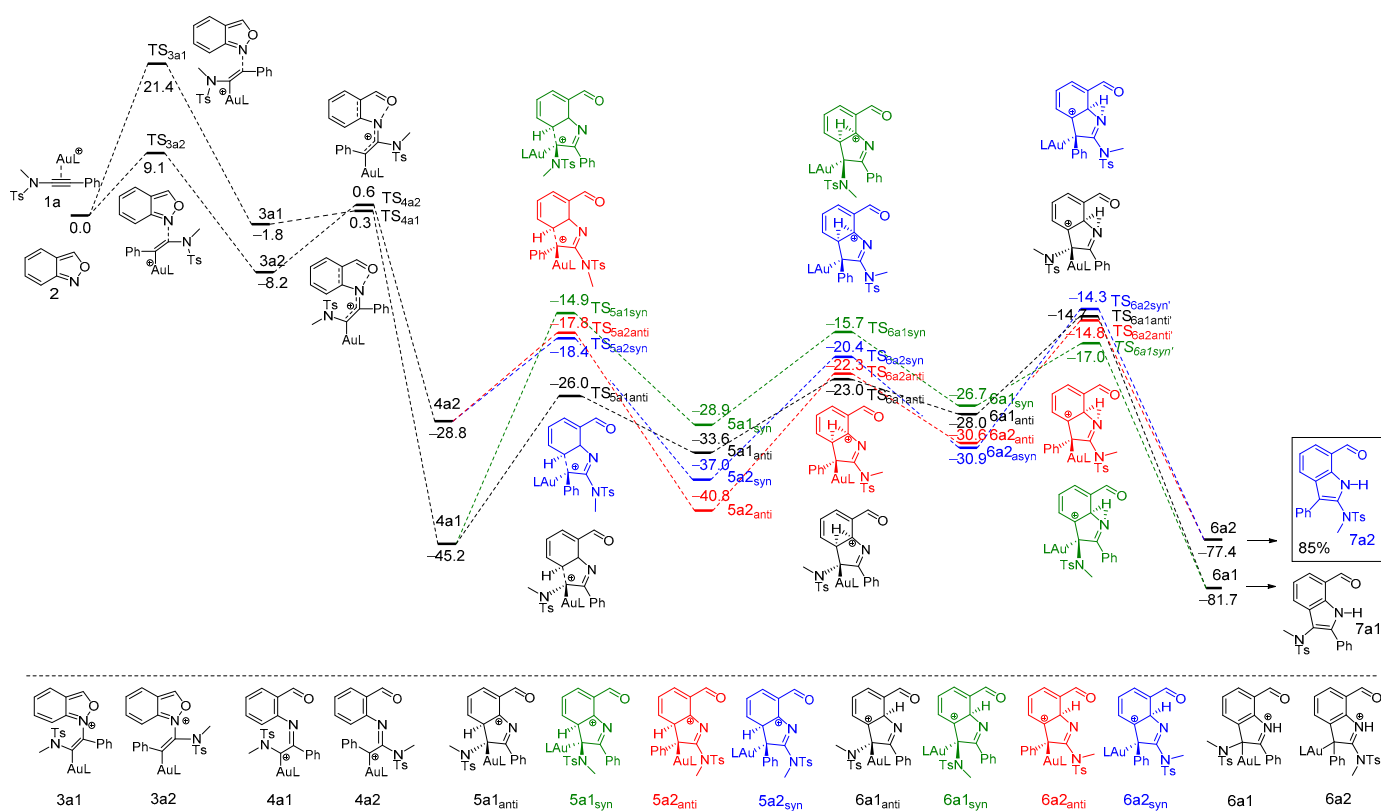
Scheme 2. Anticipated mechanistic steps for the Au(I)-mediated reaction between ynamides and oxadiazoles by analogy to that found for anthranils.

2. Results

2.1. Reaction of Anthranil with Ynamide

In our earlier approach to this chemistry, we had explored in detail the reaction between anthranil and a terminal ynamide. Given the striking power and versatility of this chemistry, in an attempt to provide a generalized view of the mechanisms involved, a side-by-side comparison between the reactivity of terminal and substituted ynamides seems appropriate.

The full profile for the substituted ynamide can be found in Scheme 3, and it compares well with that obtained earlier for the terminal ynamide [50], with regioselectivity still strongly favoring the attack on C1 compared to C2 of the gold-activated ynamide by 12.3 kcal/mol compared to the 14.8 kcal/mol observed for the terminal ynamide. The key chemical steps are the same, and the overall energy barriers are quite similar and follow the general description provided above, which involves five stages (alkyne activation, nucleophilic attack, N-O bond cleavage, cyclization, and deauration). Interestingly, the main difference when moving from a terminal to a substituted ynamide resides in the thermodynamics of the reaction. Whereas with the terminal ynamide the final and observed product is kinetically and thermodynamically favored, in the substituted ynamide the observed product is only kinetically favored (and thermodynamically less stable than the alternative regioisomer by 4.3 kcal/mol, see Scheme 3). This reversal in exergonicity, presumably, is due to the phenyl ring not being able to participate in extending the conjugation of the heterocycle in **7a2** vs. conjugated in **7a1** (Scheme 3). This situation, however, applies only insofar as the gold is complexed to the substrate, and it should not affect the reaction outcome since the steep energy drop in the N-O bond cleavage makes the process irreversible from that step onwards.



Scheme 3. Mechanistic pathway and relative free energies (kcal mol⁻¹, 298 K, and 1 Atm) for the reaction between anthranil and the ynamide MeN(Ts)≡CPh.

The key activation barriers for the mechanism depicted in Scheme 3 are summarized below (Table 1) and they show why this reaction is operative even at very mild thermal

conditions ($-20\text{ }^{\circ}\text{C}$) since the starting favored nucleophilic attack only requires 9.1 kcal/mol and a path is available such that no step requires more than 17 kcal/mol.

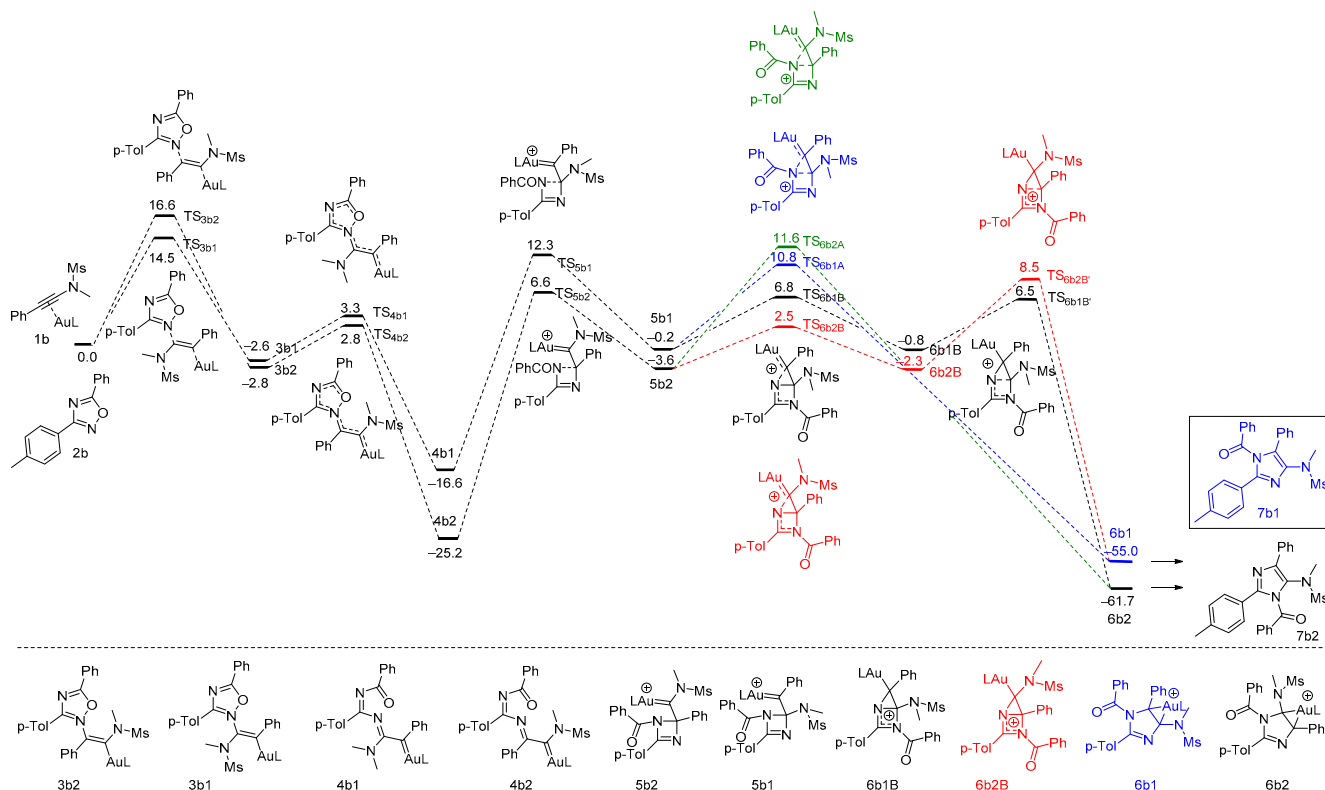
Table 1. Calculated transition states and Gibbs free energies of activation (ΔG^{\ddagger} , in kcal mol $^{-1}$) for each step of the mechanism between anthranil and ynamide MeN(Ts)C \equiv CPh.

1st Step	ΔG^{\ddagger}	2nd Step	ΔG^{\ddagger}	3rd Step	ΔG^{\ddagger}	4th Step	ΔG^{\ddagger}	5th Step	ΔG^{\ddagger}
TS _{3a1}	21.4	TS _{4a1}	2.1	TS _{5a1_anti}	19.2	TS _{6a1_anti}	10.6	TS _{6a1_anti'}	13.3
				TS _{5a1_syn}	30.3	TS _{6a1_syn}	13.2	TS _{6a1_syn'}	9.7
TS _{3a2}	9.1	TS _{4a2}	8.8	TS _{5a2_anti}	10.4	TS _{6a2_anti}	16.6	TS _{6a2_anti'}	16.6
				TS _{5a2_syn}	11.0	TS _{6a2_syn}	18.5	TS _{6a2_syn'}	15.8

2.2. Reaction of 1,2,4-Oxadiazole with Ynamide

Next, we decided to study the similarities and differences of the reaction when considering the reaction between 3-tolyl-5-diphenyl-1,2,4-oxadiazole and the internal ynamide, PhC \equiv C-N(Ms)Me. The first formal difference in this substrate is the presence of two nitrogen atoms within the heterocyclic structure; this could result in chemoselectivity issues, although, experimentally, a single isomer is formed. Therefore, upon activation of the triple bond in the ynamide by gold, the nucleophilic attack of two nitrogen centers is possible. Nitrogen at position 2, directly bonded to oxygen, is expected to be a stronger nucleophile due to lone pair repulsion or alpha effect [51]. Indeed the reaction barrier is slightly more favorable for the nucleophilic attack of N2 of the oxadiazole on the polarized alkyne (Scheme 4). Not only that, the intermediate formed in the case of the participation of N4 as nucleophile is unstable with respect to reactants (by almost 3 kcal/mol), contrary to the mildly stable intermediates formed when N2 is the attacking center (regardless of whether this attack occurs at the favored or disfavored site of the triple bond, i.e., **3b1** and **3b2**). Nevertheless, the regioselectivity of this step still favors the attack on C1 compared to C2, however the energy difference is much lower (2 kcal/mol in oxadiazole vs. 12 kcal/mol when the attack was performed by anthranil) and the activation barriers lie together halfway in between those observed for anthranil. Oxadiazole, therefore, is potentially less selective and it shows a nucleophilicity that is, on average, comparable to that of anthranil (14.9 and 16.6 kcal/mol for oxadiazole vs. 9.1 and 21.4 kcal/mol for anthranil). The second step involves the N–O bond cleavage through TS_{4b1} or TS_{4b2} with low energy barriers, 5.9 and 5.6 kcal/mol, respectively. The steep energy drop associated with this bond cleavage is dampened here with respect to what we observed with anthranil. This is mostly due to the fused benzene that is missing in this case, in anthranil part of the driving force in this step is the aromatization of this fragment from an o-quinone-like structure in the starting substrate (see **3a1** and **4a1**, for instance, in Scheme 3). An energy drop of 19.9 kcal/mol for the kinetically favorable **3b1** system is still enough to ensure irreversibility, as in the former mechanism. This cleavage leads to the α -imino gold carbene intermediates **4b1** and **4b2**, from which we expected a 5-exo-dig cyclization due to a nucleophilic attack of Bz-N on the gold-carbene. This should readily form the desired aminoimidazole ring (**7b1** in Scheme 4), however, our attempts to locate this transition state for the aminoimidazole ring formation were not successful. Unexpectedly, a four-member ring was formed through a 4-endo-trig nucleophilic attack of Bz-N on the vicinal carbon to the gold-carbon cation, with relatively high activation energies of 28.9 or 31.7 kcal/mol for TS_{5b1} or TS_{5b2}, respectively (Scheme 4 and Table 2). This unexpected result gives an explanation for the striking difference in thermal requirements for this process, compared to the previous reaction with anthranil (-20 vs. $80\text{ }^{\circ}\text{C}$). This latter step, and its associated high activation energy due to the unfavorable 4-endo-trig requirements, opens the possibility for identifying this reaction as a 4π -electron electrocyclic ring closure (vide infra). After the formation of **5b1** and **5b2** the reaction paths form a complex manifold in which a ring expansion process occurs. Interestingly, both intermediates can ring expand via two different mechanisms: (1) the *N*-imine attack onto the gold carbene and (2) the *N*-acetamide attack alternative

(labeled A in Scheme 4). The latter is less competitive for both intermediates and results in the concomitant cleavage of the C-N bond, furnishing the ring-expanded system in a single step. The *N*-imide attack (labeled B in Scheme 4) is kinetically favored, and it involves a stepwise ring expansion process through the formation of a 2.2.1 bicyclic structure, which is an actual but short-lived intermediate that readily opens to furnish the final **6b2** imidazole ring. Interestingly, this complex manifold is another regioselectivity-determining stage since it allows cross-linking of both paths. For instance, if the concerted *N*-acetamide attack could be made more favorable, the initial regioselectivity selected in the starting step (**TS**_{3b1} and **TS**_{3b2}) would be reversed and the experimentally non-observed isomer would be formed.



Scheme 4. Mechanistic pathway and relative free energies (kcal mol⁻¹, 298 K, and 1 Atm) for the reaction between 1,2,4-oxadiazole and the ynamide MeN(Ms)≡CPh.

Table 2. Calculated transition states and Gibbs free energies of activation (ΔG^\ddagger , in kcal mol⁻¹) for each step of the mechanism between 1,2,4-oxadiazoles and ynamide MeN(Ms)C≡CPh.

1st Step	ΔG^\ddagger	2nd Step	ΔG^\ddagger	3rd Step	ΔG^\ddagger	4th Step	ΔG^\ddagger	5th Step	ΔG^\ddagger
TS _{3b1}	14.5	TS _{4b1}	5.9	TS _{5b1}	28.9	TS _{6b1A}	11.0	-	-
TS _{3b2}	16.6	TS _{4b2}	5.6	TS _{5b2}	31.7	TS _{6b1B}	7.0	TS _{6b1B'}	7.3
TS _{3b3}	16.2					TS _{6b2A}	15.2	-	-
						TS _{6b2B}	6.1	TS _{6b2B'}	10.8

Due to the unexpected and rather unfavorable arrangement of the four-member ring, we decided to explore whether this step features pericyclic characteristics or if it should be described as a rather unfavorable 4-endo-dig nucleophilic attack. To do that, we looked for signature consequences of a pericyclic process, like aromaticity at the transition states [52–57]. Nucleus-independent chemical shifts were therefore computed at the four-member ring geometrical center and along an axis perpendicular to the ring. Pericyclic transition states show a bell- or double bell-shape profile for this aromaticity magnetic parameter, with maximum value(s) near the center of the ring. As can be seen in Figure 1, this is hardly

the case of the four-member ring formation. Chemical shift values are very low in the equatorial region of the ring being formed, and they only increase when moving away from the ring due to the accidental encounter with electron density from other fragments of the molecule. With these results in hand, we can safely assume that this is not a reaction of a pericyclic nature, but a fairly unfavorable nucleophilic attack.

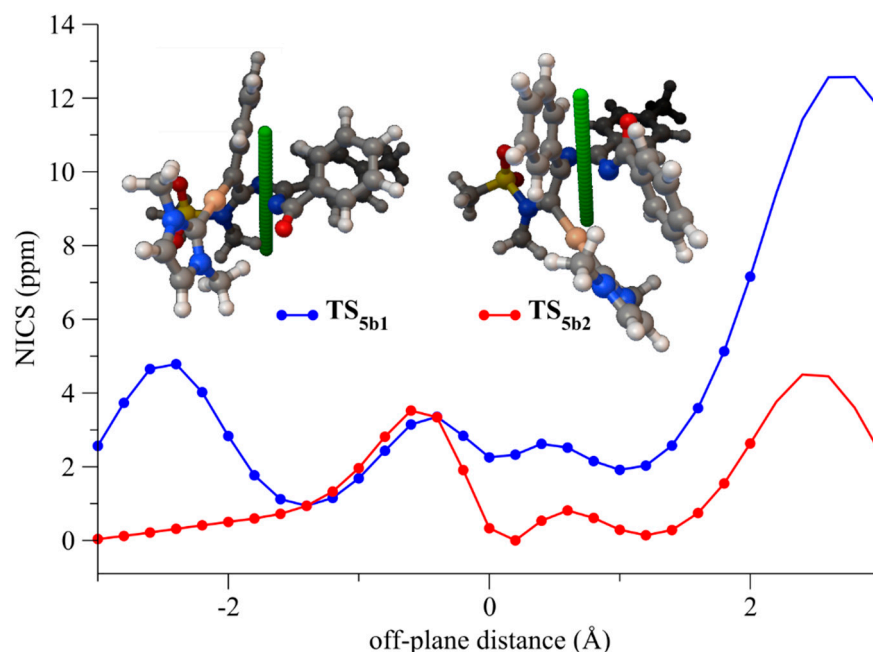
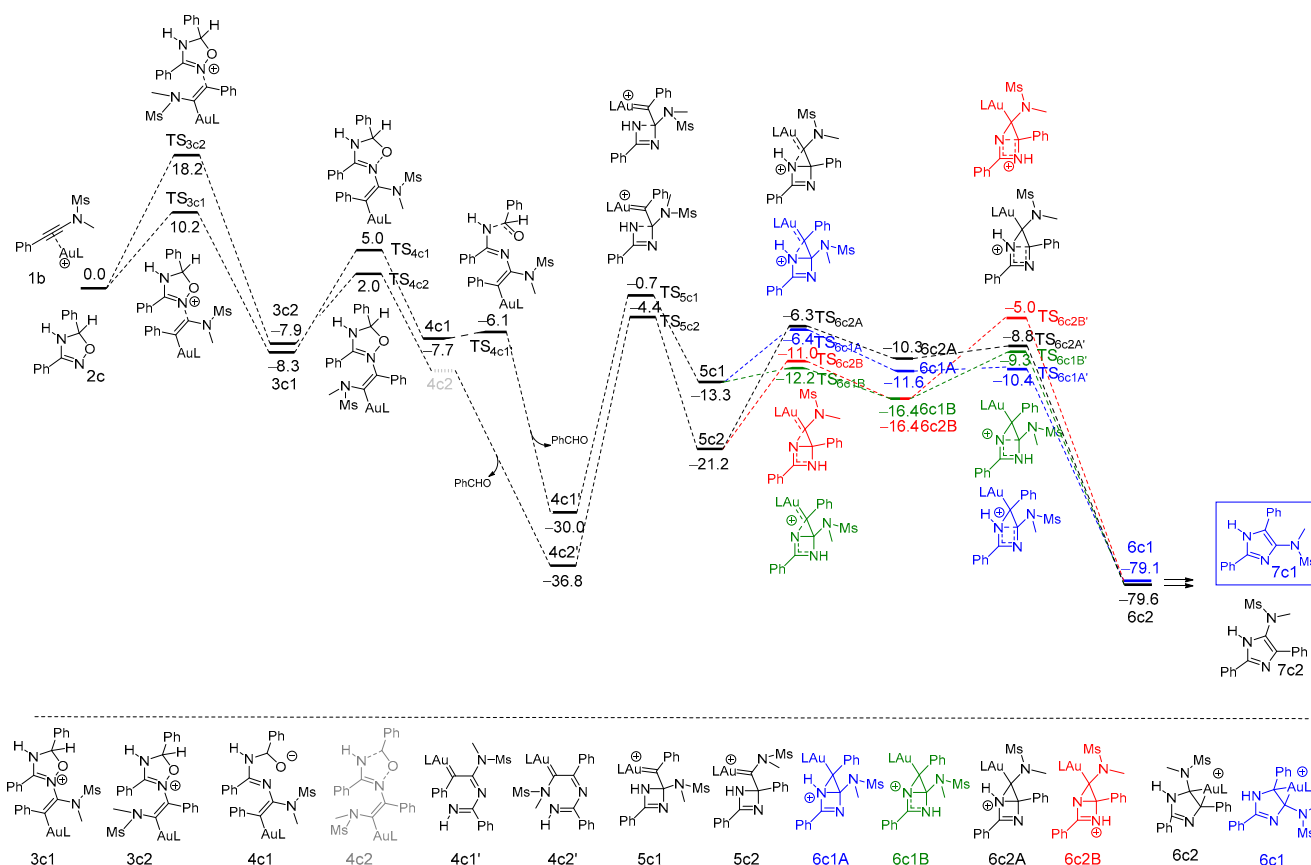


Figure 1. Nucleus-independent chemical shifts computed at the M06/Def2SVPP level for TS_{5b1} and TS_{5b2} .

2.3. Reaction of 4,5-Dihydro-1,2,4-Oxadiazole with Ynamide

Finally, we considered the pathway for the reaction between 3,5-diphenyl-4,5-dihydro-1,2,4-oxadiazole and ynamide $PhC\equiv C-N(Ms)Me$ (Scheme 5) to study how the saturation of the 4,5 N-C bond affects the reactivity. With this substrate, the starting nucleophilic attack of oxadiazole on the activated ynamide triple bond shows improved selectivity traits, comparable to that of anthranil (10.2 vs. 18.2 kcal/mol). Actually, the favored attacks for these two species show remarkably similar barriers, since the nucleophilic attack of anthranil on the C1 of an activated terminal ynamide required only 9.1 kcal/mol (the sp^3 nitrogen attack was also explored and it is uncompetitive by more than 7 kcal/mol with respect to TS_{3c1}). Then, a low activation barrier allows for N-O bond cleavage, leading to α -imino gold carbene intermediates **4c1** and **4c2**. In this instance the sole N-O cleavage does not produce a remarkable energy drop, however, it is tightly associated with the loss of benzaldehyde (in a barrierless manner for **3c2** and through a short-lived intermediate for **3c2**). Both steps combined do provide a remarkably steep drop of more than 30 kcal/mol to yield the α -imino gold carbene intermediates **4c1** and **4c2** and again ensuring irreversibility. The open substrate again undergoes a costly 4-endo-trig cyclization, which requires about 30 kcal/mol for the favored regioisomer **4c1**. This high energy barrier explains why the dehydrogenated substrate needs not only harsh temperatures, but also extended reaction times (Scheme 1). In this instance, the four-member cyclic intermediate proceeds to the ring expansion only through a stepwise process and via the formation of a short-lived 2.1.0 bicyclic intermediate. The difference in energy of activation for the imine (favored) and the amine (unfavored) attack in both paths is enough (5–6 kcal/mol, approximately) to ensure maintaining the regioselectivity obtained in the starting step although, again, reversal of this trend would also revert the regioselectivity of the process. A summary of the cost of each reaction step in this catalytic process can be found in Table 3.



Scheme 5. Mechanistic pathway and relative free energies (kcal mol⁻¹, 298 K, and 1 atm) for the reaction between 1,5-dihydro-1,2,4-oxadiazole and the ynamide MsN(Ms)≡CPh.

Table 3. Calculated transition states and Gibbs free energies of activation (ΔG^\ddagger , in kcal mol⁻¹) for each step of the mechanism between 1,5-dihydro-1,2,4-oxadiazole and the ynamide MeN(Ms)≡CPh.

1st Step	ΔG^\ddagger	2nd Step	ΔG^\ddagger	3rd Step	ΔG^\ddagger	4th Step	ΔG^\ddagger	5th Step	ΔG^\ddagger	6th Step	ΔG^\ddagger
TS _{3c1}	10.2	TS _{4c1A}	13.3	TS _{4c1B}	1.6	TS _{5c1A}	29.3	TS _{6c1A}	6.9	TS _{7c1A}	1.2
TS _{3c2}	18.2	TS _{4c2A}	9.9	TS _{4c2B}	–	TS _{5c2A}	32.4	TS _{6c1B}	1.1	TS _{7c1B}	7.1
TS _{3c3}	18.0							TS _{6c2A}	14.9	TS _{7c2A}	1.5
								TS _{6c2B}	10.2	TS _{7c2B}	11.4

3. Computational Methods

Throughout this work, the Kohn–Sham formulation of density-functional theory was employed [58,59]. The meta-hybrid density functional M06 [60] has been used with the extended double- ζ quality Def2-SVPP basis set for all the static calculations [61]. This combination of density functional and basis set has been found to provide good performance in homogeneous gold catalysis [62,63]. All geometry optimizations have been carried out using tight convergence criteria and a pruned grid for numerical integration, with 99 radial shells and 590 angular points per shell. In some challenging cases, this grid was enlarged to 175 radial shells and 974 points per shell for first row atoms and 250 shells and 974 points per shell for heavier elements. These challenging optimizations are usually associated with very soft vibrational modes (usually internal rotations). Analysis of the normal modes obtained via diagonalization of the Hessian matrix was used to confirm the topological nature of each stationary point. The wavefunction stability for each optimized structure has also been checked. Solvation effects have been taken into account variationally throughout the optimization procedures via the polarizable continuum model (PCM) [64], using

parameters for dichloromethane and taking advantage of the smooth switching function developed by York and Karplus [65]. Concerning the structures involved in these simulations (see the Supplementary Materials), we simplified the cationic gold complex employed in the experimental work using 1,3-bis-methyl-imidazol-2-ylidene gold as a simpler model of the catalyst IPrAuCl/AgNTf₂ and trimethylphosphine gold for tBuXPhosAu(MeCN)SbF₆ used in the experimental work [21,22] in order to find a balance between accuracy and computational efficiency. All the calculations performed in this work have been carried out with the Gaussian 09 program [66].

4. Conclusions

We investigated the similarities and differences in the mechanism of Au(I)-catalyzed [3 + 2] reactions between the mild nucleophiles anthranil, 3-tolyl-1,2,4-oxadiazole, or 3-phenyl-4,5-dihydro-1,2,4-oxadiazole and a highly polarized alkyne, i.e., the ynamide PhC≡C-N(Ms)Me. These reactions regioselectively produce 2-amino-3-phenyl-7-acyl indoles, *N*-acyl-5-aminoimidazoles, or *N*-*H*-5-phenyl-4-aminoimidazoles, respectively. In the proposed mechanisms, the vinyl gold intermediate evolves by the oxazole or oxadiazole ring opening to a key α -imino gold carbene complex. In all cases the regioselectivity is decided early, at the initial nucleophilic attack of N in anthranil or N2 in oxadiazole on the C1 carbon of the Au(I)-activated ynamide in combination with an energy drop during α -imino gold carbene formation. In the five-member rings, however, a late-stage reaction path manifold opens the door for regioselectivity reversal, although this is not the case in the reactions considered and tested experimentally. Such possibility is opened through an unexpected four-member ring formation, which necessitates a posterior ring expansion stage during which the C-N bond formed in the starting step may be conserved or may be broken. This late-stage mechanism manifold could therefore be exploited to steer regioselectivity towards the so far non-observed product. Our ongoing studies seek to explain via simulations the regioselectivity in reactions of anthranil with ynamides activated by various forms of gold catalyst.

Supplementary Materials: The following supporting information can be downloaded at <https://www.mdpi.com/article/10.3390/catal12080915/s1>: Solvation effects, cartesian coordinates for all the structures computed in this work, reaction profiles including discarded, non-competitive paths (Figure S1: A-series reaction mechanism; Figure S2: B-series reaction mechanism; Figure S3: C-series reaction mechanism; Figure S4: B-series reaction mechanism including the alternative path of nucleophilic attack of N-4 of 1,2,4-oxadiazole on ynamide; Figure S5: C-series reaction mechanism including the alternative path of nucleophilic attack of N-4 of 1,2,4-oxadiazole on ynamide); Table S1: values of partial charges for Series-B; Table S2: values of partial charges for Series-C; Table S3: values of partial charges on the structures of alternative cyclization for Series-B/C are provided as supporting information.

Author Contributions: Conceptualization, A.K. and C.S.L.; formal analysis, I.S., A.K., C.S.L. and I.L.; investigation, I.S. and I.L.; data curation, I.S., A.K. and I.S.; writing—original draft preparation, A.K. and I.S.; writing—review and editing, C.S.L.; supervision, A.K. and C.S.L. All authors have read and agreed to the published version of the manuscript.

Funding: This research received no external funding.

Data Availability Statement: Not applicable.

Acknowledgments: This research includes part of the PhD research of IS. AK thanks Chiesi Hellas (project 10354) for supporting this research. CSL thanks the Ministerio de Ciencia e Innovación (PID2020-115789GB-C22) and Xunta de Galicia (ED431C 2021/41), which partially funded this work. Generous allocation of supercomputer resources by CESGA is also acknowledged.

Conflicts of Interest: The authors declare no conflict of interest.

References

1. Gorin, D.J.; Davis, N.R.; Toste, F.D. Gold(I)-Catalyzed Intramolecular Acetylenic Schmidt Reaction. *J. Am. Chem. Soc.* **2005**, *127*, 11260–11261. [[CrossRef](#)] [[PubMed](#)]
2. Benitez, D.; Shapiro, N.D.; Tkatchouk, E.; Wang, Y.; Goddard, W.A.; Toste, F.D. A Bonding Model for Gold(I) Carbene Complexes. *Nat. Chem.* **2009**, *1*, 482–486. [[CrossRef](#)] [[PubMed](#)]
3. Gorin, D.J.; Toste, F.D. Relativistic Effects in Homogeneous Gold Catalysis. *Nature* **2007**, *446*, 395–403. [[CrossRef](#)] [[PubMed](#)]
4. Brouwer, H.; Stothers, J.B. ¹³C Nuclear Magnetic Resonance Studies. XX. ¹³C Shieldings of Several Allyl Alcohols. Geometric Dependence of ¹³C Shieldings. *Can. J. Chem.* **1972**, *50*, 1361–1370. [[CrossRef](#)]
5. Seidel, G.; Fürstner, A. Structure of a Reactive Gold Carbenoid. *Angew. Chemie Int. Ed.* **2014**, *53*, 4807–4811. [[CrossRef](#)] [[PubMed](#)]
6. Seidel, G.; Mynott, R.; Fürstner, A. Elementary Steps of Gold Catalysis: NMR Spectroscopy Reveals the Highly Cationic Character of a “Gold Carbenoid”. *Angew. Chemie Int. Ed.* **2009**, *48*, 2510–2513. [[CrossRef](#)]
7. Marion, N.; Nolan, S.P. N-Heterocyclic Carbenes in Gold Catalysis. *Chem. Soc. Rev.* **2008**, *37*, 1776–1782. [[CrossRef](#)]
8. Dorel, R.; Echavarren, A.M. Gold(I)-Catalyzed Activation of Alkynes for the Construction of Molecular Complexity. *Chem. Rev.* **2015**, *115*, 9028–9072. [[CrossRef](#)]
9. Hong, F.-L.; Ye, L.-W. Transition Metal-Catalyzed Tandem Reactions of Ynamides for Divergent N-Heterocycle Synthesis. *Acc. Chem. Res.* **2020**, *53*, 2003–2019. [[CrossRef](#)]
10. Chen, Y.-B.; Qian, P.-C.; Ye, L.-W. Brønsted Acid-Mediated Reactions of Ynamides. *Chem. Soc. Rev.* **2020**, *49*, 8897–8909. [[CrossRef](#)]
11. Luo, J.; Chen, G.-S.; Chen, S.-J.; Yu, J.-S.; Li, Z.-D.; Liu, Y.-L. Exploiting Remarkable Reactivities of Ynamides: Opportunities in Designing Catalytic Enantioselective Reactions. *ACS Catal.* **2020**, *10*, 13978–13992. [[CrossRef](#)]
12. Hu, Y.-C.; Zhao, Y.; Wan, B.; Chen, Q.-A. Reactivity of Ynamides in Catalytic Intermolecular Annulations. *Chem. Soc. Rev.* **2021**, *50*, 2582–2625. [[CrossRef](#)] [[PubMed](#)]
13. Shandilya, S.; Protim Gogoi, M.; Dutta, S.; Sahoo, A.K. Gold-Catalyzed Transformation of Ynamides. *Chem. Rec.* **2021**, *21*, 4123–4149. [[CrossRef](#)] [[PubMed](#)]
14. Madhavan, S.; Keshri, S.K.; Kapur, M. Transition Metal-Mediated Functionalization of Isoxazoles: A Review. *Asian J. Org. Chem.* **2021**, *10*, 3127–3165. [[CrossRef](#)]
15. Gao, Y.; Nie, J.; Huo, Y.; Hu, X.-Q. Anthranils: Versatile Building Blocks in the Construction of C–N Bonds and N-Heterocycles. *Org. Chem. Front.* **2020**, *7*, 1177–1196. [[CrossRef](#)]
16. Aguilar, E.; Santamaría, J. Gold-Catalyzed Heterocyclic Syntheses through α -Imino Gold Carbene Complexes as Intermediates. *Org. Chem. Front.* **2019**, *6*, 1513–1540. [[CrossRef](#)]
17. Zhao, X.; Rudolph, M.; Asiri, A.M.; Hashmi, A.S.K. Easy Access to Pharmaceutically Relevant Heterocycles by Catalytic Reactions Involving α -Imino Gold Carbene Intermediates. *Front. Chem. Sci. Eng.* **2020**, *14*, 317–349. [[CrossRef](#)]
18. Zeng, Z.; Jin, H.; Sekine, K.; Rudolph, M.; Rominger, F.; Hashmi, A.S.K. Gold-Catalyzed Regiospecific C–H Annulation of *o*-Ethylnylbiaryls with Anthranils: π -Extension by Ring-Expansion En Route to N-Doped PAHs. *Angew. Chemie Int. Ed.* **2018**, *57*, 6935–6939. [[CrossRef](#)]
19. Zeng, Z.; Jin, H.; Rudolph, M.; Rominger, F.; Hashmi, A.S.K. Gold(III)-Catalyzed Site-Selective and Divergent Synthesis of 2-Aminopyrroles and Quinoline-Based Polyazaheterocycles. *Angew. Chemie Int. Ed.* **2018**, *57*, 16549–16553. [[CrossRef](#)]
20. González, J.; Santamaría, J.; Suárez-Sobrino, Á.L.; Ballesteros, A. One-Pot and Regioselective Gold-Catalyzed Synthesis of 2-Imidazolyl-1-Pyrazolylbenzenes from 1-Propargyl-1 H -Benzotriazoles, Alkynes and Nitriles through α -Imino Gold(I) Carbene Complexes. *Adv. Synth. Catal.* **2016**, *358*, 1398–1403. [[CrossRef](#)]
21. Zeng, Z.; Jin, H.; Xie, J.; Tian, B.; Rudolph, M.; Rominger, F.; Hashmi, A.S.K. α -Imino Gold Carbenes from 1,2,4-Oxadiazoles: Atom-Economical Access to Fully Substituted 4-Aminoimidazoles. *Org. Lett.* **2017**, *19*, 1020–1023. [[CrossRef](#)] [[PubMed](#)]
22. Xu, W.; Wang, G.; Sun, N.; Liu, Y. Gold-Catalyzed Formal [3 + 2] Cycloaddition of Ynamides with 4,5-Dihydro-1,2,4-Oxadiazoles: Synthesis of Functionalized 4-Aminoimidazoles. *Org. Lett.* **2017**, *19*, 3307–3310. [[CrossRef](#)] [[PubMed](#)]
23. Rani, N.; Sharma, A.; Singh, R. Trisubstituted Imidazole Synthesis: A Review. *Mini Rev. Org. Chem.* **2014**, *12*, 34–65. [[CrossRef](#)]
24. Strelnikova, J.O.; Rostovskii, N.V.; Starova, G.L.; Khlebnikov, A.F.; Novikov, M.S. Rh(II)-Catalyzed Transannulation of 1,2,4-Oxadiazole Derivatives with 1-Sulfonyl-1,2,3-Triazoles: Regioselective Synthesis of 5-Sulfonamidoimidazoles. *J. Org. Chem.* **2018**, *83*, 11232–11244. [[CrossRef](#)]
25. Ermolat’ev, D.S.; Van der Eycken, E.V. A Divergent Synthesis of Substituted 2-Aminoimidazoles from 2-Aminopyrimidines. *J. Org. Chem.* **2008**, *73*, 6691–6697. [[CrossRef](#)]
26. Guo, X.; Chen, W.; Chen, B.; Huang, W.; Qi, W.; Zhang, G.; Yu, Y. One-Pot Three-Component Strategy for Functionalized 2-Aminoimidazoles via Ring Opening of α -Nitro Epoxides. *Org. Lett.* **2015**, *17*, 1157–1159. [[CrossRef](#)]
27. Guchhait, S.K.; Hura, N.; Shah, A.P. Synthesis of Polysubstituted 2-Aminoimidazoles via Alkene-Diamination of Guanidine with Conjugated α -Bromoalkenones. *J. Org. Chem.* **2017**, *82*, 2745–2752. [[CrossRef](#)]
28. Francini, C.M.; Fallacara, A.L.; Artusi, R.; Mennuni, L.; Calgani, A.; Angelucci, A.; Schenone, S.; Botta, M. Identification of Aminoimidazole and Aminoimidazole Derivatives as Src Family Kinase Inhibitors. *ChemMedChem* **2015**, *10*, 2027–2041. [[CrossRef](#)]
29. Francini, C.M.; Musumeci, F.; Fallacara, A.L.; Botta, L.; Molinari, A.; Artusi, R.; Mennuni, L.; Angelucci, A.; Schenone, S. Optimization of Aminoimidazole Derivatives as Src Family Kinase Inhibitors. *Molecules* **2018**, *23*, 2369. [[CrossRef](#)]
30. Bennett, L.L., Jr.; Baker, H.T. Synthesis of Potential Anticancer Agents. IV. 4-Nitro- and 4-Amino-5-Imidazole Sulfones. *J. Am. Chem. Soc.* **1957**, *79*, 2188–2191. [[CrossRef](#)]

31. Zhang, L.; Brodney, M.A.; Candler, J.; Doran, A.C.; Duplantier, A.J.; Efremov, I.V.; Evrard, E.; Kraus, K.; Ganong, A.H.; Haas, J.A.; et al. 1-[(1-Methyl-1H-Imidazol-2-yl)methyl]-4-Phenylpiperidines as MGlur2 Positive Allosteric Modulators for the Treatment of Psychosis. *J. Med. Chem.* **2011**, *54*, 1724–1739. [[CrossRef](#)] [[PubMed](#)]
32. Mehrabi, H.; Alizadeh-Bami, F.; Meydani, A.; Besharat, S. An Eco-Friendly Approach for the Synthesis of 1,2,5-Trisubstituted and 4-Amino-1,2,5-Tetrasubstituted Imidazoles via a Multi-Component Condensation. *Arkivoc* **2021**, *2021*, 86–95. [[CrossRef](#)]
33. Hashmi, A.S.K. Introduction: Gold Chemistry. *Chem. Rev.* **2021**, *121*, 8309–8310. [[CrossRef](#)] [[PubMed](#)]
34. Mato, M.; Franchino, A.; García-Morales, C.; Echavarren, A.M. Gold-Catalyzed Synthesis of Small Rings. *Chem. Rev.* **2021**, *121*, 8613–8684. [[CrossRef](#)]
35. Reyes, R.L.; Iwai, T.; Sawamura, M. Construction of Medium-Sized Rings by Gold Catalysis. *Chem. Rev.* **2021**, *121*, 8926–8947. [[CrossRef](#)] [[PubMed](#)]
36. Wang, T.; Hashmi, A.S.K. 1,2-Migrations onto Gold Carbene Centers. *Chem. Rev.* **2021**, *121*, 8948–8978. [[CrossRef](#)]
37. Zheng, Z.; Ma, X.; Cheng, X.; Zhao, K.; Gutman, K.; Li, T.; Zhang, L. Homogeneous Gold-Catalyzed Oxidation Reactions. *Chem. Rev.* **2021**, *121*, 8979–9038. [[CrossRef](#)]
38. Hendrich, C.M.; Sekine, K.; Koshikawa, T.; Tanaka, K.; Hashmi, A.S.K. Homogeneous and Heterogeneous Gold Catalysis for Materials Science. *Chem. Rev.* **2021**, *121*, 9113–9163. [[CrossRef](#)]
39. Wang, W.; Ji, C.-L.; Liu, K.; Zhao, C.-G.; Li, W.; Xie, J. Dinuclear Gold Catalysis. *Chem. Soc. Rev.* **2021**, *50*, 1874–1912. [[CrossRef](#)]
40. Zhou, A.-H.; He, Q.; Shu, C.; Yu, Y.-F.; Liu, S.; Zhao, T.; Zhang, W.; Lu, X.; Ye, L.-W. Atom-Economic Generation of Gold Carbenes: Gold-Catalyzed Formal [3 + 2] Cycloaddition between Ynamides and Isoxazoles. *Chem. Sci.* **2015**, *6*, 1265–1271. [[CrossRef](#)]
41. Zhang, Y.; Luo, T.; Yang, Z. Strategic Innovation in the Total Synthesis of Complex Natural Products Using Gold Catalysis. *Nat. Prod. Rep.* **2014**, *31*, 489–503. [[CrossRef](#)]
42. Campeau, D.; León Rayo, D.F.; Mansour, A.; Muratov, K.; Gagosz, F. Gold-Catalyzed Reactions of Specially Activated Alkynes, Allenes, and Alkenes. *Chem. Rev.* **2021**, *121*, 8756–8867. [[CrossRef](#)]
43. Rocchigiani, L.; Bochmann, M. Recent Advances in Gold(III) Chemistry: Structure, Bonding, Reactivity, and Role in Homogeneous Catalysis. *Chem. Rev.* **2021**, *121*, 8364–8451. [[CrossRef](#)] [[PubMed](#)]
44. Lu, Z.; Li, T.; Mudshinge, S.R.; Xu, B.; Hammond, G.B. Optimization of Catalysts and Conditions in Gold(I) Catalysis-Counterion and Additive Effects. *Chem. Rev.* **2021**, *121*, 8452–8477. [[CrossRef](#)] [[PubMed](#)]
45. Chintawar, C.C.; Yadav, A.K.; Kumar, A.; Sancheti, S.P.; Patil, N.T. Divergent Gold Catalysis: Unlocking Molecular Diversity through Catalyst Control. *Chem. Rev.* **2021**, *121*, 8478–8558. [[CrossRef](#)]
46. Ye, L.-W.; Zhu, X.-Q.; Sahani, R.L.; Xu, Y.; Qian, P.-C.; Liu, R.-S. Nitrene Transfer and Carbene Transfer in Gold Catalysis. *Chem. Rev.* **2021**, *121*, 9039–9112. [[CrossRef](#)]
47. Melekhova, A.A.; Smirnov, A.S.; Novikov, A.S.; Panikorovskii, T.L.; Bokach, N.A.; Kukushkin, V.Y. Copper(I)-Catalyzed 1,3-Dipolar Cycloaddition of Ketonitrones to Dialkylcyanamides: A Step toward Sustainable Generation of 2,3-Dihydro-1,2,4-Oxadiazoles. *ACS Omega* **2017**, *2*, 1380–1391. [[CrossRef](#)]
48. Breugst, M.; Reissig, H.U. The Huisgen Reaction: Milestones of the 1,3-Dipolar Cycloaddition. *Angew. Chem. Int. Ed.* **2020**, *59*, 12293–12307. [[CrossRef](#)]
49. Ess, D.H.; Houk, K.N. Distortion/Interaction Energy Control of 1,3-Dipolar Cycloaddition Reactivity. *J. Am. Chem. Soc.* **2007**, *129*, 10646–10647. [[CrossRef](#)]
50. Stylianakis, I.; Litinas, I.; Nieto Faza, O.; Kolocouris, A.; Silva López, C. On the Mechanism of the Au(I)-Mediated Addition of Alkynes to Anthranils to Furnish 7-Acylindoles. *J. Phys. Org. Chem.* **2022**, e4333. [[CrossRef](#)]
51. Hansen, T.; Vermeeren, P.; Bickelhaupt, F.M.; Hamlin, T.A. Origin of the α -Effect in S_N2 Reactions. *Angew. Chemie Int. Ed.* **2021**, *60*, 20840–20848. [[CrossRef](#)]
52. Schleyer, P.V.R.; Maerker, C.; Dransfeld, A.; Jiao, H.; van Eikema Hommes, N.J.R. Nucleus-Independent Chemical Shifts: A Simple and Efficient Aromaticity Probe. *J. Am. Chem. Soc.* **1996**, *118*, 6317–6318. [[CrossRef](#)] [[PubMed](#)]
53. Moll, J.F.; Pemberton, R.P.; Gutierrez, M.G.; Castro, C.; Karney, W.L.J. Configuration Change in [14]Annulene Requires Möbius Antiaromatic Bond Shifting. *Am. Chem. Soc.* **2007**, *129*, 274–275. [[CrossRef](#)] [[PubMed](#)]
54. Fallah-Bagher-Shaidaei, H.; Wannere, C.S.; Corminboeuf, C.; Puchta, R.; Schleyer, P.V.R. Which NICS Aromaticity Index for Planar π Rings Is Best? *Org. Lett.* **2006**, *8*, 863–866. [[CrossRef](#)] [[PubMed](#)]
55. Chen, Z.; Wannere, C.S.; Corminboeuf, C.; Puchta, R.; Schleyer, P. von R. Nucleus-Independent Chemical Shifts (NICS) as an Aromaticity Criterion. *Chem. Rev.* **2005**, *105*, 3842–3888. [[CrossRef](#)] [[PubMed](#)]
56. Morao, I.; Cossio, F.P. A Simple Ring Current Model for Describing In-Plane Aromaticity in Pericyclic Reactions. *J. Org. Chem.* **1999**, *64*, 1868–1874. [[CrossRef](#)]
57. López, C.S.; Nieto Faza, O.; Freindorf, M.; Kraka, E.; Cremer, D. Solving the Pericyclic–Pseudopericyclic Puzzle in the Ring-Closure Reactions of 1,2,4,6-Heptatetraene Derivatives. *J. Org. Chem.* **2016**, *81*, 404–414. [[CrossRef](#)]
58. Hohenberg, P.; Kohn, W. Inhomogeneous Electron Gas. *Phys. Rev.* **1964**, *136*, 864–871. [[CrossRef](#)]
59. Kohn, W.; Sham, L.J. Self-Consistent Equations Including Exchange and Correlation Effects. *Phys. Rev.* **1965**, *140*, 1133–1138. [[CrossRef](#)]
60. Zhao, Y.; Truhlar, D.G. The M06 Suite of Density Functionals for Main Group Thermochemistry, Thermochemical Kinetics, Noncovalent Interactions, Excited States, and Transition Elements: Two New Functionals and Systematic Testing of Four M06-Class Functionals and 12 Other Function. *Theor. Chem. Acc.* **2008**, *120*, 215–241. [[CrossRef](#)]

61. Bauernschmitt, R.; Ahlrichs, R.J. Stability Analysis for Solutions of the Closed Shell Kohn-Sham Equation. *Chem. Phys.* **1996**, *104*, 9047–9052. [[CrossRef](#)]
62. Faza, O.N.; Rodríguez, R.Á.; López, C.S. Performance of Density Functional Theory on Homogeneous Gold Catalysis. *Theor. Chem. Acc.* **2011**, *128*, 647–661. [[CrossRef](#)]
63. Faza, O.; López, C. Computational approaches to homogeneous gold catalysis. *Top. Curr. Chem.* **2014**, *357*, 213–283.
64. Tomasi, J.; Mennucci, B.; Cammi, R. Quantum Mechanical Continuum Solvation Models. *Chem. Rev.* **2005**, *105*, 2999–3094. [[CrossRef](#)] [[PubMed](#)]
65. York, D.M.; Karplus, M.J. A Smooth Solvation Potential Based on the Conductor-like Screening Model. *Phys. Chem. A* **1999**, *103*, 11060–11079. [[CrossRef](#)]
66. Frisch, M.J.; Trucks, G.W.; Schlegel, H.B.; Scuseria, G.E.; Robb, M.A.; Cheeseman, J.R.; Scalmani, G.; Barone, V.; Mennucci, B.; Petersson, G.A.; et al. *Gaussian 09*; Gaussian, Inc.: Wallingford, CT, USA, 2009.